APPLIED GEOPHYSICS, Vol.14, No.1 (March 2017), P. 31-39, 7 Figures.
DOI:10.1007/s11770-017-0608-y

Rock-physics models of hydrate-bearing sediments in permafrost, Qilian Mountains, China*

Liu Jie[1], Liu Jiang-Ping♦[1], Cheng Fei[1], Wang Jing[1], and Liu Xiao-Xiao[1]

Abstract: Rock-physics models are constructed for hydrate-bearing sediments in the Qilian Mountains permafrost region using the K–T equation model, and modes I and II of the effective medium model. The K–T equation models the seismic wave propagation in a two-phase medium to determine the elastic moduli of the composite medium. In the effective medium model, mode I, the hydrate is a component of the pore inclusions in mode I and in mode II it is a component of the matrix. First, the P-wave velocity, S-wave velocity, density, bulk modulus, and shear modulus of the sediment matrix are extracted from logging data.. Second, based on the physical properties of the main components of the sediments, rock-physics model is established using the K–T equation, and two additional rock-physics models are established assuming different hydrate-filling modes for the effective medium. The model and actual velocity data for the hydrate-bearing sediments are compared and it is found that the rock-physics model for the hydrate-filling mode II well reproduces the actual data.
Keywords: Hydrates, rock-physics, seismic wave velocity, density, porosity

Introduction

In 2008, hydrates were first discovered in the Qilian Mountains permafrost (Zhu et al., 2009). Presently, there is a wealth of data regarding the hydrate-bearing sediments in the permafrost of Qilian Mountains, such as depth, thickness, velocity, and density. Hydrate-bearing sediments occur in fissures in siltstones and mudstones, and in the pores of sandstones. The pores are a major reservoir for hydrates, and it is possible to calculate the porosity and hydrate saturation based on density, acoustic data, and resistivity data (Lu et al., 2010; Zhu et al., 2010; Pang et al., 2012). Using exploration data for hydrates in the permafrost region of Qilian Mountains, we build a rock-physics model for permafrost hydrates. Hydrate samples were collected from boreholes DK-1, DK-2, DK-3, and DK-4 in the Qilian Mountains permafrost region. Borehole DK-4 did not yield hydrate samples; however, there were particles similar to hydrate crystals in the drilling mud. Bubbles were observed in cores at 115.0–150.0 m and 162.0–163.0 m in borehole DK-4 as well as ignition of gas. The first core section comprises siltstone, fine-grained sandstone, and mudstone, and the reservoir space is made of pores and fissures. The second core section core comprises siltstone and reservoir pore space (Zhu et al., 2010; Lu et al., 2010). The logging data for borehole DK-4 show the characteristic high resistivity

Manuscript received by the Editor August 3, 2016; revised manuscript received March 22, 2017
*This work was supported by the Institute of Geophysical and Geochemical Exploration (IGGE) CAGS of China (No. WH201207).
1. Institute of Geophysics and Geomatics, China University of Geosciences, Wuhan 430074, China.
♦Corresponding author: Liu Jiang-Ping (Email: liujp_geop@126.com)

and high velocity associated with hydrates in fine-grained sandstone and siltstone at 130.4–132.3 m and 165.3–167.3 m (Guo, 2011). The 115.0–170.0 m interval in borehole DK-4 lies in a fault zone (Pang et al., 2012); therefore, the fracture density is high and cementation is poor. It is inferred that several sections of borehole DK-4 contain hydrates. In this study, we focus on reservoir porosity models using data from the hydrate reservoirs, and types of pores and fractures.

Zimmerman and King (1986) used the K–T equation to construct a rock-physics model for hydrate-bearing sediments. Lee et al. (1996) used the three-phase time-averaged equation to build a model, without considering the elastic moduli of the sediments. Helgerud et al. (1999) constructed a rock-physics model and estimated the concentration of hydrates from velocity models at the Blake–Bahama Ridge in southeastern United States, but this method has not yet been applied to hydrate-bearing sediments in permafrost regions. Using data for the Blake Ridge area and microstructures, Dai et al. (2004) analyzed the filling modes of the pore space of hydrate-bearing sediments in permafrost regions. Shankar et al. (2013) used elasticity theory to analyze hydrate-bearing sediments and estimated the hydrate saturation using velocity predictions velocity that were consistent with the in situ velocity from the Krishna-Godavari Basin in eastern India. Song et al. (2002) and Sun et al. (2003) calculated the P- and S-wave velocity using the elastic moduli of hydrate-bearing sediments. Hu et al. (2010) investigated micromodels of hydrates in different types of sediments and the effect of hydrates on the acoustic properties in consolidated and unconsolidated sediments. Li and Chen (2013) constructed rock-physics models to account for the seismic wave propagation in pores that are generally mm or smaller than the 10 m to 100 m scale of the seismic wavelength. Li et al. (2014) analyzed the relation between saturation and permeability of gas hydrates in the South China Sea, where the permeability of the hydrate-bearing sediments is assumed good. When the hydrate saturation is high, most of the pore spaces are filled, and the hydrate particles are bonded with rock particles. This is the cementation model (Tang et al., 2016). The hydrate particles are treated as part of the matrix in this model. Muhammed et al. (2016) constructed a rock-physics model using the effective medium model and fluid substitution theory to analyze the offshore seismic AVO characteristics in the Makran accretionary prism, Pakistan. Sell et al. (2016) used X-ray tomography to observe the formation of hydrates in the pores of artificial cores and found that the hydrates were present in a variety of states, including hydrate particles not in contact with the rock particles and suspended in fluids, hydrate particles in contact with rock particles, and hydrate cemented with rock particles. Therefore, hydrates are part of the pore filling and part of the matrix in hydrate-bearing sediments. The physical properties of hydrate-bearing sediments depend on the main components (hydrates, water, and sandstone) and the hydrate-filling modes of the sediment pores. In addition, if the elastic moduli of hydrate-bearing sediments vary, the velocity of the hydrate-bearing sediments will also vary.

We evaluated the predicted and actual velocities to choose appropriate rock-physics models for hydrate-bearing sediments in the Qilian Mountains permafrost region. We first describe the K–T equation model and the elastic moduli model. Then, we obtain physical data for selected drilling intervals and calculate the physical parameters of the hydrates. Finally, the different rock-physics models for hydrates are assessed using the differences between the theoretical and actual velocity data for the hydrate-bearing sediments.

Rock-physics modeling

K–T equation model

The K–T equation model is based on two components, the matrix and the inclusions. We use the K–T equation to model sediments that can be described as a three-component system, e.g., hydrate, water, and sandstone (Kuster et al., 1974; Lee et al., 1996). The pore shapes in K–T equation models are spherical, discoid, and needle- and coin-like, and each shape has a corresponding modulus. However, because the cores from the Qilian Mountains permafrost were not maintained under the proper temperatures and pressures, the pore shapes of the hydrate-bearing sediments were not obtained. In the macroscopic simulation of the strata, the pore shape of the hydrate-bearing sediments is assumed uniformly ellipsoidal. As the figure 1 shows the model moduli and velocity are computed by the following procedure.

First, we compute the bulk modulus K_1 and the shear modulus G_1 of mixture (a), in which the hydrates are the matrix and water the inclusions. The volume ratio of hydrate to water is $S/(1 - S)$. The K_1 and G_1 of the two-component mixture (a) are calculated using equation (1) (Kuster and Toksöz, 1974).

Second, we compute the bulk modulus K_2 and shear modulus G_2 of mixture (b), in which the sandstone constitutes the matrix and mixture (a) forms the

inclusions. The K_2 and G_2 of the three-component mixture (b) are calculated using equation (2) (Kuster and Toksöz, 1974).

Third, once the bulk modulus and shear modulus are known, and the bulk density has been calculated using equation (3), the P-wave velocity (v_p) and S-wave velocity (v_s) are calculated with equation (4).

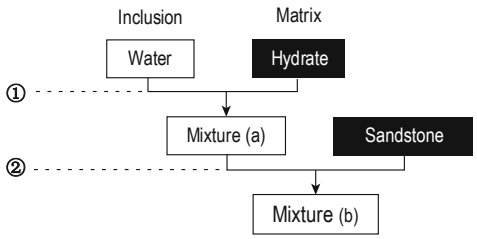

Fig.1 K–T equation model for calculating the bulk modulus and shear modulus of a three-phase mixture.

$$\begin{cases} K_1 = K_h \cdot \dfrac{1+[4G_h(K_w-K_h)/((3K_w+4G_h)/K_h)](1-S)}{1-[3(K_w-K_h)/(3K_w+4G_h)](1\text{-}S)} \\ G_1 = G_h \cdot \dfrac{(6K_h+12G_h)G_w + (9K_h+8G_h)[SG_h+(1-S)G_w]}{(9K_h+8G_h)G_h + (6K_h+12G_h)[SG_w+(1-S)G_h]} \end{cases}, \quad (1)$$

$$\begin{cases} K_2 = K_m \cdot \dfrac{1+[4G_m(K_1-K_m)/((3K_1+4G_m)/K_m)]\phi}{1-[3(K_1-K_m)/(3K_1+4G_m)]\phi} \\ G_2 = G_m \cdot \dfrac{(6K_m+12G_m)G_1 + (9K_m+8G_m)[(1-\phi)G_m+\phi G_1]}{(9K_m+8G_m)G_m + (6K_m+12G_m)[(1-\phi)G_1+\phi G_m]} \end{cases}, \quad (2)$$

$$\rho = (1-S)\phi\rho_w + S\phi\rho_h + (1-\phi)\rho_m, \quad (3)$$

where ρ is the bulk density, ρ_w is the water density, ρ_h is the hydrate density, and ρ_m is the sandstone density, Φ is the porosity, S is the hydrate saturation, and K_w, K_h, K_m and G_w, G_h, and G_m are the bulk and shear modulus of water, hydrate, and rock matrix.

$$\begin{cases} v_p = \sqrt{\dfrac{(K_2+4G_2/3)}{\rho}} \\ v_s = \sqrt{\dfrac{G_2}{\rho}} \end{cases}, \quad (4)$$

Effective medium model with different filling modes

The hydrate-bearing sediments are modeled using the different filling modes of the effective medium model (Helgerud et al., 1999; Ecker, 2001; Dai et al., 2004). In mode I, the hydrate particles are suspended in the pore fluids or the loose contacts between hydrate particles and sand grains; therefore, the hydrates are part of the pore inclusions. In mode II, the contacts between hydrate particles and sand grains are closed or cemented; therefore, the hydrates are matrix components.

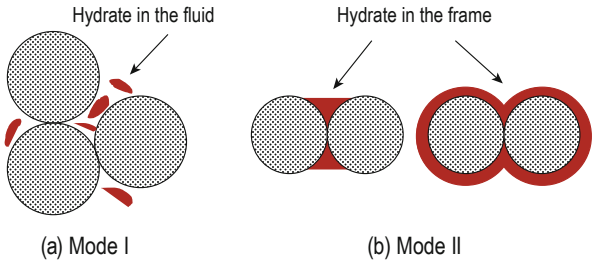

Fig.2 Hydrate-filling modes I and II (Dvorkin and Nur, 1996), where the circles represent the sand grains and the red shade the hydrate.
(a) Mode I, the hydrate particles are suspended in the pore fluids and are part of the pore inclusions. (b) Mode II, the contacts between hydrate particles and sand grains are close or cemented and the hydrate is part of the matrix.

Mode I

In mode I, the hydrate is a component of the pore inclusions and affects the fluid elastic properties. The calculation of the effective medium model involves several parameters and related coefficients. The P- and S-wave velocity of the hydrate model are calculated with the following equations

$$\begin{cases} v_p = \sqrt{\dfrac{K_{sat}+\dfrac{4}{3}G_{sat}}{\rho}} \\ v_s = \sqrt{\dfrac{G_{sat}}{\rho}} \end{cases}, \quad (5)$$

where K_{sat} and G_{sat} are the bulk and shear modulus of the fluid-saturated sediments, and the bulk density ρ is calculated with equation (3).

We obtain K_{sat} and G_{sat} for the hydrate model using equations (6)–(11), where Φ is the porosity, K_n and G_n are the bulk and shear modulus of the rock matrix,

respectively, calculated with equation (7), K_f is the bulk modulus of the pore inclusions calculated with equation (8), and K_{dry} and G_{dry} are the bulk and shear modulus of the dry rock matrix calculated with equation (9).

$$\begin{cases} K_{sat} = K_n \dfrac{\phi K_{dry} - (1+\phi)K_f K_{dry}/K_n + K_f}{(1-\phi)K_f + \phi K_n - K_f K_{dry}/K_n} \\ G_{sat} = G_{dry} \end{cases}, \quad (6)$$

$$\begin{cases} K_n = \dfrac{1}{2}[\sum_{i=1}^{N} f_i K_i + (\sum_{i=1}^{N} \dfrac{f_i}{K_i})^{-1}] \\ G_n = \dfrac{1}{2}[\sum_{i=1}^{N} f_i G_i + (\sum_{i=1}^{N} \dfrac{f_i}{G_i})^{-1}] \end{cases}, \quad (7)$$

where N is the number of matrix components, K_i and G_i are the bulk and shear modulus of the i-th component, and f_i is the volume percentage of the i-th component. In mode I, the matrix contains a single component; therefore, N is equal to 1, and K_1 and G_1 represent the bulk and shear modulus of the rock matrix.

In equations (8) and (9), K_h is the hydrate bulk modulus, K_w is the water bulk modulus, S_h is the hydrate saturation, and S_w is the water saturation. The bulk modulus K_f of the pore inclusions is

$$K_f = [\frac{S_h}{K_h} + \frac{S_w}{K_w}]^{-1}, \quad (8)$$

$$\begin{cases} K_{dry} = [\dfrac{\phi/\phi_c}{K_{hm} + \frac{4}{3}G_{hm}} + \dfrac{1-\phi/\phi_c}{K_n + \frac{4}{3}G_{hm}}]^{-1} - \dfrac{4}{3}G_{hm} \\ G_{dry} = [\dfrac{\phi/\phi_c}{G_{hm} + Z} + \dfrac{1-\phi/\phi_c}{G_{hm} + Z}]^{-1} - Z \end{cases}, \quad (9)$$

In equation (9), Φ_c is the critical porosity of 40% (Dvorkin and Nur, 1996; Helgerud et al., 1999). The porosity of the hydrate-bearing sediments from the Qilian Mountain permafrost region is generally not greater than 10%. Parameter Z is

$$Z = \frac{G_{hm}}{6(9K_{hm} + 8G_{hm})/(K_{hm} + 2G_{hm})}, \quad (10)$$

$$\begin{cases} K_{hm} = [\dfrac{K_n^2 k^2 (1-\phi_c)^2}{18\pi^2(1-\sigma)^2} P]^{1/3} \\ G_{hm} = \dfrac{5-\sigma}{5(2-\sigma)}[\dfrac{3G_n^2 k^2 (1-\phi_c)^2}{2\pi^2(1-\sigma)^2} P]^{1/3} \end{cases}, \quad (11)$$

where K_{hm} and G_{hm} are the bulk and shear modulus of the rock with critical porosity, and σ is the Poisson's ratio of the rock matrix in equation (12), P is the effective pore pressure calculated with equation (13), in which ρ_m is the matrix density, h is the sediment depth, and g is the gravitational acceleration (9.8 m/s^2).

$$\sigma = \frac{3K_n - 2G_n}{2(3K_n + G_n)}, \quad (12)$$

$$P = (1-\phi)(\rho_m - \rho_w)gh. \quad (13)$$

Parameter k is the average number of contact points per grain (Murphy et al., 1982; Shankar et al., 2013)

$$k = 15 - 34\phi + 14\phi^2. \quad (14)$$

In Figure 3a, the number of contacts per grain is no more than three in unconsolidated sands, and the porosity is high. In Figure 3b, the number of contacts per grain is four to six, the porosity is relatively high, and the contacts are compact. In Figure 3c, the number of contacts per grain is more than seven, the porosity is very low, and the contacts are highly compact. It is possible to calculate the value of k from the porosity; for example, for Φ =10%, the value of k is 11.7 from equation (14).

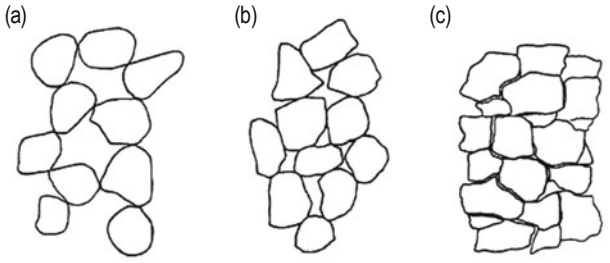

Fig.3 Contact structures in granular matrix (Murphy, 1982).
(a) Three or fewer contacts per grain; (b) four to six contacts per grain; (c) more than seven contacts per grain.

Mode II

In mode II, the hydrate is a component of the matrix. The velocities of hydrate-bearing sediments are calculated; however, some of the calculation steps are modified. The hydrate becomes a component of the rock matrix instead of the pore inclusions; thus, we recalculate the elastic modulus of the matrix and inclusions.

There is only water in the pores of mode II hydrate-bearing sediments, and hence the bulk modulus K_f is

equal to K_w, and the porosity adjusts to $\Phi(1 - S_h)$. The rock matrix contains two solid components, hydrate and sand, with volume of f_h and f_s, respectively

$$\begin{cases} f_s = (1-\phi)/(1-\phi') \\ f_h = \phi S_h / (1-\phi') \end{cases}. \quad (15)$$

In mode II, the value of N is adjusted to 2 to calculate the elastic moduli from equation (7), in which K_1 and G_1 are the bulk and shear modulus of the sandstone and K_2 and G_2 are the bulk and shear modulus of the hydrate. The velocity calculation of mode II is almost the same as that of mode I, but the calculation of the elastic modulus is modified to account for the different hydrate-filling modes.

Rock properties

To construct a hydrate rock-physics model, it is necessary to know the physical parameters of the three major components of the hydrate-bearing sediments. The physical parameters for hydrate and water are the wave velocities, density, and elastic moduli (Table 1). The physical parameters of the rock matrix are calculated based on actual data from hydrate-bearing sediments in the Qilian Mountains permafrost region.

Table 1 Elastic constants for hydrate and water (Lee et al., 1996; Shankar et al., 2013)

Component	v_p (m/s)	v_s (m/s)	ρ (g/cm^3)	K (Gpa)	G (Gpa)
Hydrate	3300	1680	0.90	6.40	2.55
Water	1500	0	1.01	2.25	0

Data from the hydrate-bearing sediments at 165.80 to 166.35 m depth in borehole DK-4 are used to construct the model (Table 2). Because of the lack of shear-wave velocity data, we cannot directly estimate the elastic moduli of the rock matrix. Thus, we first try to calculate the velocity ratio to obtain the S-wave velocity. Borehole DK-1 is situated 250 m southwest of borehole DK-4, and the hydrate-bearing interval at depth 143.40–144.20 m in borehole DK-1 and depth 165.80–166.35 m in borehole DK-4 belong to the same sedimentary system (Zhu et al., 2009, 2010; Lu et al., 2010; Pang et al., 2012). The two intervals are both pink sandstone (Guo, 2011); therefore, we consider the velocity ratios of the rock matrix of the hydrate-bearing sediments equivalent. If the velocity ratio of borehole DK-1 is known, then, the S-wave velocity of the equivalent borehole DK-4 interval is calculated according to the following steps.

1. In borehole DK-1, the P-wave velocity and S-wave velocity of the hydrate-bearing sedimentary matrix are calculated from the time-averaged equation that is used to obtain the velocity ratio (v_p/v_s), which is used as the velocity ratio of the hydrate-bearing sedimentary matrix in borehole DK-4.

2. In borehole DK-4, the P-wave velocity and density of the matrix are calculated from the time-averaged equation. Once the velocity ratio is known from step 1, the S-wave velocity of borehole DK-4 matrix is calculated.

3. From the relation between elastic moduli and velocity, we obtain the bulk and shear moduli of the hydrate-bearing sedimentary matrix in borehole DK-4.

Table 2 Data for hydrate-bearing sediments at 165.80–166.35 m in borehole DK-4 (Guo, 2011)

Depth (m)	Φ (%)	S (%)	P (g/cm^3)	v_p (m/s)
165.80	8.97	54.24	2.22	3865
165.85	8.36	57.37	2.22	3849
165.90	7.90	59.71	2.22	3850
165.95	7.61	61.19	2.22	3866
166.00	7.49	61.82	2.22	3890
166.05	7.52	61.64	2.22	3916
166.10	7.70	60.71	2.22	3936
166.15	8.00	59.18	2.22	3945
166.20	8.37	57.30	2.22	3945
166.25	8.74	55.42	2.22	3937
166.30	9.04	53.88	2.22	3927
166.35	9.24	52.89	2.22	3919
Average	8.67	55.76	2.22	3815

Table 3 Data for hydrate-bearing sediments at 143.40–144.20 m in borehole DK-1 (Zhu et al., 2009; Guo, 2011)

Φ (%)	S (%)	ρ (g/cm^3)	v_p (m/s)	v_s (m/s)	v_p / v_s
1.30	73.50	2.37	4688	2354	1.991

The velocity, density, and elastic moduli of the matrix in the hydrate-bearing sediments for borehole DK-4 are listed in Table 4. The calculations and related equations are described in appendix A.

Table 4 Properties of the hydrate-bearing sediments matrix in borehole DK-4

v_{mp} (m/s)	v_{ms} (m/s)	ρ_m (g/cm^3)	K_m (Gpa)	G_m (Gpa)
4198	2116	2.33	27.2	10.5

Rock-physics modeling results

Rock-physics modeling of the hydrate-bearing sediments is carried out using the K–T equation and the effective medium theory. The porosity of the borehole DK-4 hydrate-bearing interval (165.80–166.35 m) is 7–10% and the saturation is between 50% and 62% (Table 2). It is considered that the hydrate-bearing sediments satisfy the conditions for applying the K–T equation, because the main pore space of the formation being filled with hydrate comes from the low porosity and the high hydrate saturation. In addition, poor consolidation and loose structure are observed at the borehole DK-4 hydrate-bearing interval, where the F25 fault zone is and small faults are observed in the core (Pang et al., 2012). Moreover, the geological conditions and structures of the hydrate-bearing sediments also apply to the effective media model for different filling modes.

The P- and S-wave velocities are calculated with the K–T equation, and modes I and II of the effective medium model. The model porosity is 15%, the hydrate saturation ranges from 0% to 80%, and the properties of the components (velocity, density, and elastic moduli) in Tables 1 and 4 are used. The P- and S-wave velocities are shown in Figure 4 for the K–T equation, mode I, and mode II. The velocity of each model varies similarly. When the hydrate saturation is constant, the velocity decreases with increasing porosity and when the porosity is constant, the velocity significantly increases with increasing saturation. The different models show similar velocity variations for porosity and hydrate saturation, but the magnitude of the velocity variation differs.

The P- and S-wave velocities and the ratio of P- to S-wave velocity for 15% porosity and hydrate saturation of 0% to 80% are shown in Figures 4 and 5. For a given porosity, the P-wave velocity is highest for the K–T equation and lowest for mode I. The S-wave velocity varies similarly, but increases very slowly with increasing saturation for mode I. With increasing saturation, the velocity ratios of the K–T equation are nearly constant, but the velocity ratios of mode I and mode II markedly increase. For the same values of parameters, the three models differ in the P- and S-wave velocity; K–T equation yields the highest values, mode I the lowest, and mode II is in the middle.

The velocity data for the K–T equation, mode I, and mode II are compared with the actual velocity data for hydrate-bearing sediments in borehole DK-4. The actual velocity data are from 12 sampling points (Table 2), with porosity values of 7.49–9.24% and hydrate saturation

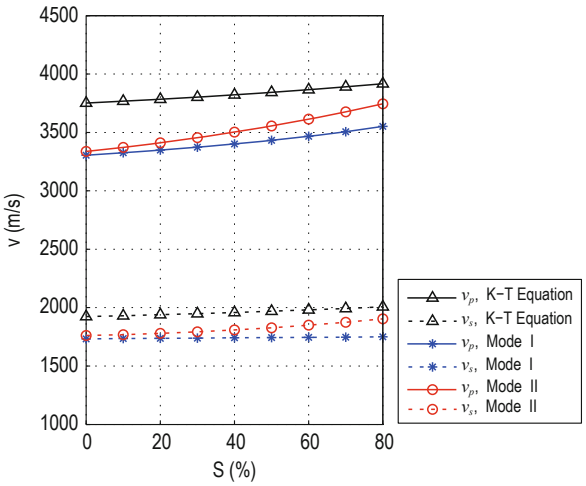

Fig.4 P- and S-wave velocity calculated with the K–T equation, mode I, and mode II. Each model velocity varies similarly but the magnitude is different.

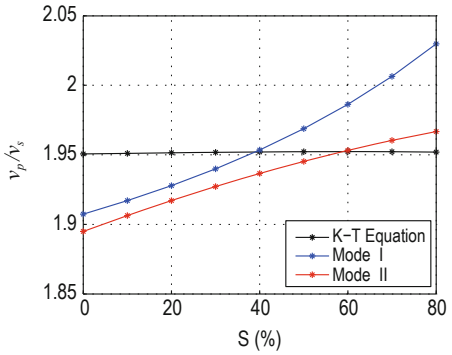

Fig.5 Ratios of P-wave to S-wave velocity for the three models and 15% porosity.

of 52.89–61.82%. Based on porosity of 10% and 7% and saturation of 0–80%, the calculated velocities for the three models are shown in Figure 6. The black, blue, and red lines represent the velocity of the K–T equation, mode I, and mode II, respectively. The black dots denote the actual velocity data, and the lines with triangles and circles denote the curves for 7% and 10% porosity, respectively. To assess which model better reflects the actual physical properties of the hydrate-bearing sediments, the differences between the model velocity and the actual velocity data are evaluated.

In Figure 6, the black dots denoting the actual data are located below the K–T equation velocity curve. Half of the black dots fall within the area between the two blue curves and most of the black dots are located between the two red curves. The velocities calculated with the K–T equation and the model deviate from the actual data, but mode II is closer to the actual data. Thus, by comparing the model and actual velocities for the 165.80

–166.35 m interval in borehole DK-4, we find that mode II best reflects the actual velocity data . We speculate that the hydrate particles are not suspended in the pore fluids but are part of the rock matrix and are in close contact with the rock grains or are cemented.

For building the hydrate rock-physics model, the volume fractions and elastic moduli of the main constituents must be known as well as the geometrical structure (Mavko et al., 2003). The K–T equation is simplified (Kuster and Toksöz, 1974) and ignores the geometrical structure of the main constituents in the formation. The effective model with the Gassmann formula is used to account for the structural characteristics of the inclusions, and depends on the hydrate particles that are considered as inclusions and the matrix that separately interacts with the rock particles, which is closer to the actual hydrate-filling and geometric patterns in the pores. By comparing the two rock-physics modeling methods, the effective models of the different modes can reproduce the physical properties. Both models suggest that seismic velocity increases with increasing hydrate saturation; however, the K–T model is simple and inaccurate, and the effective model is slightly more complex to calculate.

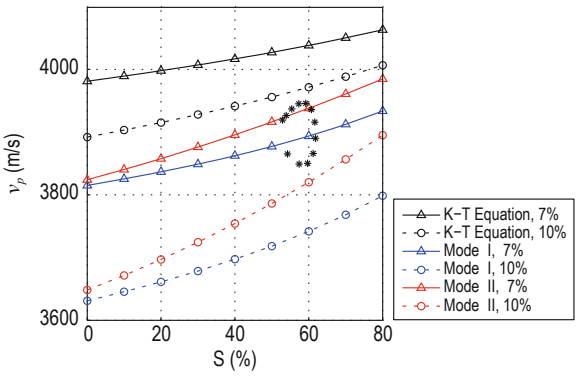

Fig.6 Predicted and actual velocity data at the 165.80–166.35 m interval of borehole DK-4.

The black, blue, and red lines represent the velocity of the K–T equation, mode I, and mode II, respectively. The lines with triangles and circles denote the curves for 7% and 10% porosity, and the black dots denote the actual velocity data.

The exploration of the Qilian Mountains permafrost hydrates is currently at the early stage and adequate logging and drilling data are not available; therefore, we cannot determine whether all hydrate-bearing sediments display filling mode II. It is possible that there are hydrate-bearing sediments with filling mode I but further work is needed.

When the number of contacts per grain (k) varies, the velocities calculated with the mode II equation also vary. We assume that k and Φ (porosity) are not directly related, and the P-wave velocity is calculated for k equal to 4, 7, and 10 and Φ of 7% and 10%, as shown in Figure 7. For fixed porosity and saturation, k is associated with high greater P-wave velocity. Because, we cannot get the k values of the hydrate-bearing sediments in the Qilian Mountain permafrost zone, we calculate the k values with equation (14) using model porosities. The porosities of the hydrate-bearing sediments are between 7% and 10% in borehole DK-4 and correspond to k values between 11.7 and 12.7. Clearly, the hydrate-bearing sediments are relatively dense, with hydrate particles and sand grains in proximity or cemented, which suggests the hydrate-bearing sediments in borehole DK-4 belong to mode II of the effective medium model.

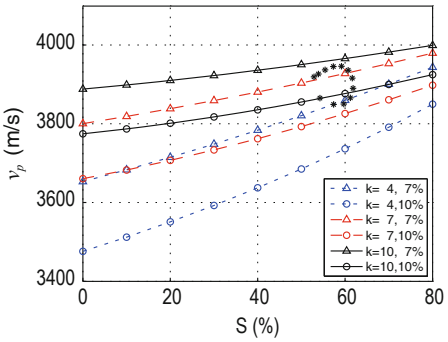

Fig.7 Calculated P-wave velocity for different k values (the number of contacts per grain) using the mode II equation of the effective medium model. Values of k are 4, 7, and 10 and porosity Φ is 7% and 10%.

Conclusions

The mode II rock-physics model of hydrate-bearing sediments produces results closest to the actual values at the 165.80–166.35 m depth interval in borehole DK-4. Regarding the hydrates as component of the rock matrix better reflects the actual properties of hydrate-containing sediments. The rock-physics model based on the K–T equation is a mixture of the main components in the formation and does not consider the hydrates filling the pores. The effective medium model with filling modes I and II makes up for this deficiency and better simulates hydrate-bearing sediments. In the future, we will expand the database by considering additional geological data, as they become available.

Acknowledgments

We are grateful for the support of the Institute of Geophysical and Geochemical Exploration (IGGE) CAGS. We also thank the reviewers and editors for their comments and valuable suggestions, and appreciate their help. Best wishes for everyone.

Reference

Dai, J., Xu, H. B., Snyder, F., and Dutta, N., 2004, Detection and estimation of gas hydrates using rock physics and seismic inversion: Examples from the northern deep-water Gulf of Mexico: The leading edge, **23**(1), 60–66.

Dvorkin, J. P., and Nur, A. M., 1996, Elasticity of high-porosity sandstones: Theory for two North Sea datasets: Geophysics, **61**(5), 1363–1370.

Ecker, C., 2001, Seismic Characterization of Methane Hydrate Structures, US: Stanford University, 68–72.

Guo, X. W., 2011, Well logging Response Characteristics and Evaluation of Gas hydrae in Qilian mountain permafrost, Beijing: Chinese Academy of Geological Science, 33–42.

Helgerud, M. B., Dvorkin, J., Nur, A., Sakai, A., and Collett, T., 1999, Elastic-wave velocity in marine sediments with gas hydrates: Effective medium modeling: Geophy. Res., **26**(13), 2021–2024.

Hu, G. W., Ye, Y. G., Zhang, J., et al., 2010, Micro-models of gas hydrate and their impact on the acoustic properties of the host sediments: Natural gas industry, **30**(3), 120–124.

Kuster, G. T., and Toksöz, M. N., 1974, Velocity and attenuation of seismic waves in two-phase media-1: Geophysics, **39**, 587–606.

Lee, M. W., Hutchinson, D. R., and Dillon, W. P., 1996, Seismic velocities for hydrate-bearing sediments using weighted equation: J. Geophys. Res., **101**(B9), 20347–20358.

Li, C. H., Zhao, Q., Xu, H. J., et al., 2014, Relation between relative permeability and hydrate saturation in Shenhu area, south china sea: Applied Geophysics, **11**(2), 207–214.

Li, J. Y., and Chen, X. H., 2013, A rock-physical modeling method for carbonate reservoirs at seismic scale: Applied geophysics, **10**(1), 1–13.

Lu, Z. Q., Zhu, Y. H., Zhang, Y. Q., et al., 2010, Basic geological characteristics of gas hydrate in Qilian Mountain permafrost area, Qinghai Province: Mineral deposits, **29**(1), 182–191.

Mavko, G., Mukerji, T., and Dvorkin, J., 2003, The rock physics handbook: tools for seismic analysis of porous media, Cambridge University Press.

Muhammed, I. E., Nisar, A., Perceiz, K., et al., 2016, An application of rock physics modeling to quantify the seismic response of gas hydrate-bearing sediments in Makran accretionary prism, offshore, Pakistan: Geosciences Journal, **20**(3), 321–330.

Murphy, W. F. I., 1982, Effects of microstructure and pore fluids on the acoustic properties of granular sedimentary materials: Ph. D thesis stanford Univ., 144–147.

Pang, S. J, Su, X., He, H., et al., 2012, Geological controlling factors of gas hydrate occurrence in Qilian Mountain permafrost, China: Earth Science Frontiers, **19**(1), 1–17.

Sell, K., Saenger, E. H., Falenty, A., et al., 2016, On the path to the digital rock physics of gas hydrate bearing sediments-processing of in-situ synchrotron-tomography data: Solid Earth, **7**, 1243–1258.

Shankar, U., Gupta, D. K., Bhowmick, D., and Sain, K., 2013, Gas hydrate and free gas saturations using rock physics modeling at site NGHP-01-05 and 07 in the Krishna-Godavari Basin, eastern Indian margin: Journal of Petroleum Science and Engineering, **106**(6), 62–70.

Song, H. B., Matsubayasgi, O., Yang, S. X., et al., 2002, Physical property models of gas hydrate-bearing Sediments and AVA character of bottom simulating reflector: Chinese J. Geophys. (in Chinese), **45**(4), 546–556.

Sun, C. Y., Zhang M. Y., Niu, B. H., et al., 2003, Micro-models of gas hydrate and their velocity estimation methods: Earth science Frontiers, **10**(1), 191–198.

Tang, J., Wang, H., Yao, Z. A., et al., 2016, Shear wave velocity estimation based on rock physics diagnosis: Oil geophysical prospecting, **51**(3), 537–543.

Zimmerman, R. W., and King, M. S., 1986, The effect of the extent of freezing on seismic velocities in unconsolidated permafrost: Geophysics, **51**(6), 1285–1290.

Zhu, Y. H., Zhang, Y. Q., Wen, H. J., et al., 2009, Gas hydrates in the Qilian mountain permafrost, Qinghai, northwest China: Acta Geologica Sinica, **83**(11), 1763–1772.

Zhu, Y. H., Zhang, Y. Q., Wen, H. J., et al., 2010, Gas hydrate in the Qilian mountain permafrost and their basic characteristics: Acta Geoscientica Sinica, **31**(1), 7–16.

Appendix A

In the 143.40 m to 144.20 m depth interval in borehole DK-1, the hydrate-bearing sediments comprise sandstone, water, and hydrate. The three-phase time-averaged equation is used to analyze the hydrate-bearing sediments. The P-wave velocity of the rock matrix (v_{mp}) is

$$v_{mp} = (1-\phi)\left(\frac{1}{v_p} - \frac{(1-S)\phi}{v_w} - \frac{S\phi}{v_h}\right)^{-1}, \quad \text{(A1)}$$

where v_{mp} is the matrix velocity, vw is the water velocity, vh is the hydrate velocity, v_p is the bulk velocity, Φ is the porosity, and S is the hydrate saturation. The values for these parameters are listed in Tables 1 and 2.

The S-wave velocity in the rock matrix is

$$v_{ms} = \frac{v_{mp}}{1-\phi}\left[\frac{1}{R} - r_w\phi(1-S) - r_h\phi S\right], \quad \text{(A2)}$$

where R is the velocity ratio in borehole DK-1 and rw and rh are the velocity ratios for water and hydrates, respectively, from Table 1.

Once the matrix P-wave velocity has been calculated using equation (A1) and the S-wave velocity has been obtained using equation (A2), it is possible to calculate the ratio of P- to S-wave velocity, which is the P- to S-wave velocity ratio of the hydrate-bearing sediments matrix in borehole DK-4.

Based on the physical parameters of the hydrate-bearing sediments at the 165.80 m to 166.35 m depth interval in borehole DK-4, the matrix P-wave velocity is 4198 m/s, and the matrix S-wave velocity is equal to 2116 m/s, and the velocity ratio is 1.980.

The matrix density of hydrate-bearing sediments in borehole DK-4 is

$$\rho_m = \frac{\rho - \rho_w\phi(1-S) - \rho_h\phi S}{1-\phi}, \quad \text{(A3)}$$

where ρ is the bulk density, ρ_w, ρ_h, and ρ_m are the densities of water, hydrates, and matrix, respectively, in Table 1, and Φ and S are given in Table 2.

From the P- and S-wave velocities and the density of the matrix, the bulk and shear modulus (K_m and G_m) are

$$K_m = \rho_m\left(v_{mp}^2 - \frac{4}{3}v_{ms}^2\right), \quad \text{(A4)}$$

$$G_m = \rho_m v_{ms}^2. \quad \text{(A5)}$$

Liu Jie, is a post-doctor who received his Ph.D. degree of geodetection and information technology from China University of Geosciences (Wuhan) in 2015. His main interests are rock physics and seismic wave propagation in hydrate-bearing sediments. Email: ljky2008@126.com